El Niño–Southern Oscillation Impact on Rainfall in Uruguay

GABRIEL PISCIOTTANO*

Department of Atmospheric Sciences, University of California, Los Angeles, Los Angeles, California

ALVARO DÍAZ AND GABRIEL CAZES

Instituto de Mecánica de los Fluídos e Ingeniería Ambiental, Universidad de la República, Montevideo, Uruguay

CARLOS R. MECHOSO

Department of Atmospheric Sciences, University of California, Los Angeles, Los Angeles, California

(Manuscript received 25 May 1993, in final form 5 November 1993)

ABSTRACT

The relationships between rainfall over Uruguay (in southeastern South America) and the El Niño–Southern Oscillation phenomenon are investigated. Long time series of data from a dense network of rainfall stations are analyzed using an empirical method based on that proposed by Ropelewski and Halpert. The spatial patterns of the relationships and their temporal variability for the entire region and four subregions are studied in detail.

It is found that years with El Niño events tend to have higher than average rainfall, especially from November to the next January. Further, years with high values of the Southern Oscillation index (SOI) tend to have lower than average rainfall, especially from October through December. These findings are in general agreement with previous studies. It is also found that the period from March through July tends to have higher than average rainfall after El Niño years and lower than average rainfall after high-SOI years. For the southern part of Uruguay, the wet anomalies during El Niño events are relatively weak, but the dry anomalies during high-SOI events are significant for the two periods identified. The dry anomalies disappear, and even reverse, during January and February after high-SOI years. This feature does not have a symmetric counterpart during January and February after El Niño years.

This study, therefore, provides both a verification and an extension of other studies that have emphasized southeastern South America but have used data from only a very few stations in the region.

1. Introduction

In this paper we use data reported by a large number of rainfall stations to search for relationships between the Southern Oscillation (SO) phenomenon and precipitation anomalies in Uruguay. Our objectives are twofold:

1) To provide further validation of the results presented in previous studies by using an independent dataset. This validation is of interest because the dataset used in those studies includes very few stations in southeastern South America (C. F. Ropelewski 1992, personal communication). Only one of these stations—Montevideo—is in Uruguay, which covers a large part of the region. Montevideo's records might reflect both large-scale and local effects due to its location along the coast of Río de La Plata and its proximity to the Atlantic Ocean.

2) To assess whether there are significant subregional features in these relationships. This assessment is of interest if the relationships are to be used in long-range weather forecasting.

We focus on the extreme phases of the SO, as identified by the El Niño (EN) years defined by Rasmusson and Carpenter (1983) and the high SO index (HSOI) years defined by Ropelewski and Jones (1987). Our approach is based on the methodology used in Ropelewski and Halpert (1986, 1987, 1989; hereafter RH86, RH87, and RH89). The selected methodology is applied to long time series of rainfall data from a dense network of stations. First, we investigate whether Uruguay behaves as a coherent region in terms of rainfall anomalies during both EN and HSOI years. RH89 assume that the regions with coherent rainfall anomalies for the high-SO phase coincide with those found by RH87 for the EN phase. In a recent study, however, Halpert and Ropelewski (1992) report that each phase

* On leave from Instituto de Mecánica de los Fluídos e Ingeniería Ambiental, Universidad de la República, Montevideo, Uruguay.

Corresponding author address: Dr. Gabriel Pisciottano, University of California, Department of Atmospheric Sciences, 405 Hilgard Avenue, Los Angeles, CA 90024-1565.

of the SO is associated with surface temperature anomalies in different regions of South America. Second, we investigate the timings of the rainfall anomalies associated with each extreme phase of the SO. Last, we explore the possibility of regional differences between these anomalies.

We start in section 2 with a review of studies on the subject. Section 3 presents the data used and describes selected features of the climate of Uruguay. Sections 4 and 5 outline the methodology for analysis and show the principal results obtained in this study. A summary and discussion of those results are presented in section 6.

2. Background

There are several studies that report associations between precipitation anomalies and the extreme phases of the SO in a region of southeastern South America comprising southern Brazil, Uruguay, and northeastern Argentina (hereafter called SSA). RH87 and RH89 show that rainfall in SSA tends to be higher than average from November through the following February during EN years, and lower than average from June through December during HSOI years.

Aceituno (1988, 1991) finds that rainfall during November–December in a region similar to SSA is negatively correlated with the SOI [see Fig. 9f in Aceituno (1988)]. He also finds that the streamflow of the Paraná River tends to be negatively correlated with the SOI. The tendency for either higher or lower than average streamflow is statistically significant at the 95% level for different periods of the seasonal cycle: December of years with warm SST events, as well as January, April, and May of the following year, but not during February and March; November–December of years with cold SST events, as well as March of the following year, but not during January and February. Note that connections break in late summer during both warm and cold events.

Kiladis and Diaz (1989) analyze the *difference* in rainfall between warm and cold events for each of the three-month-long *standard seasons.* Their results confirm that in SSA the period from September through November is more rainy during warm events than during cold SST events. They also find hints of similar behavior in a small region of eastern Argentina during the periods December through February and March through May.

Mechoso and Pérez (1992) study the relationships between the SO and streamflow of two rivers in SSA: the Uruguay and Negro Rivers. They find a clear tendency for the streamflow of both the Negro and Uruguay Rivers for the period June through December in HSOI years to be below average. They also find a slight tendency for streamflow of both the Negro and Uruguay Rivers for the period November in EN years to the next February to be above average. These results provide an indirect confirmation to those obtained by RH87, RH89, and Aceituno (1988), although the relationship between rainfall and streamflow is not a simple one.

Bidegain and Caffera (1989a) find that rainfall stations in the northern, central, and western parts of Uruguay report the largest number of days with measurable precipitation during July of EN years, and the smallest during July of the previous year, with a 99% significance level. These same authors (Bidegain and Caffera 1989b) find that monthly precipitation for northwestern and central Uruguay is positively correlated with monthly mean SST in the eastern equatorial Pacific Ocean. The correlation coefficients are relatively small—albeit significant—for lags of 4 to 5 months.

Lau and Sheu (1988) find that the first empirical orthogonal function (EOF1) of the annual precipitation anomaly index has a dipole-type configuration over South America. The time evolution of the first principal component (PC1) indicates that years with a warm equatorial Pacific are strongly associated with negative values of PC1 and wet conditions in southern South America. This finding is consistent with several of the results reviewed in this paper for SSA, as well as with results obtained for Chile in southwestern South America (e.g., see Pittock 1980; Rutllant and Fuenzalida 1991).

3. Data, some climatic highlights, and interannual variability

a. Data

The data used herein are monthly precipitation reported by 99 stations (see Fig. 1) until 1980. This dataset was compiled by the Instituto de Mecánica de los Fluídos e Ingeniería Ambiental (IMFIA) at the Universidad de la República in Montevideo, Uruguay, from data obtained by the Dirección Nacional de Meteorología del Uruguay, Montevideo, which has been reporting since 1883, the longest record for an individual station. There are 30 stations that are reported since 1906. The most recent report used corresponds to December 1980. To obtain the results presented in section 4, we use the longest available time series for all stations. In section 5, we use the records from Montevideo and those from the 86 stations with records that start before or in 1914.

b. Climatic highlights and interannual variability of precipitation

Figure 2 shows contour plots of annual mean precipitation for Uruguay as well as the monthly means for January and July. The differences between the summer (January) and winter (July) patterns shown in Fig. 2 are emphasized in Fig. 3, which shows the annual cycle of monthly mean precipitation and corresponding standard deviation for three selected stations. Accord-

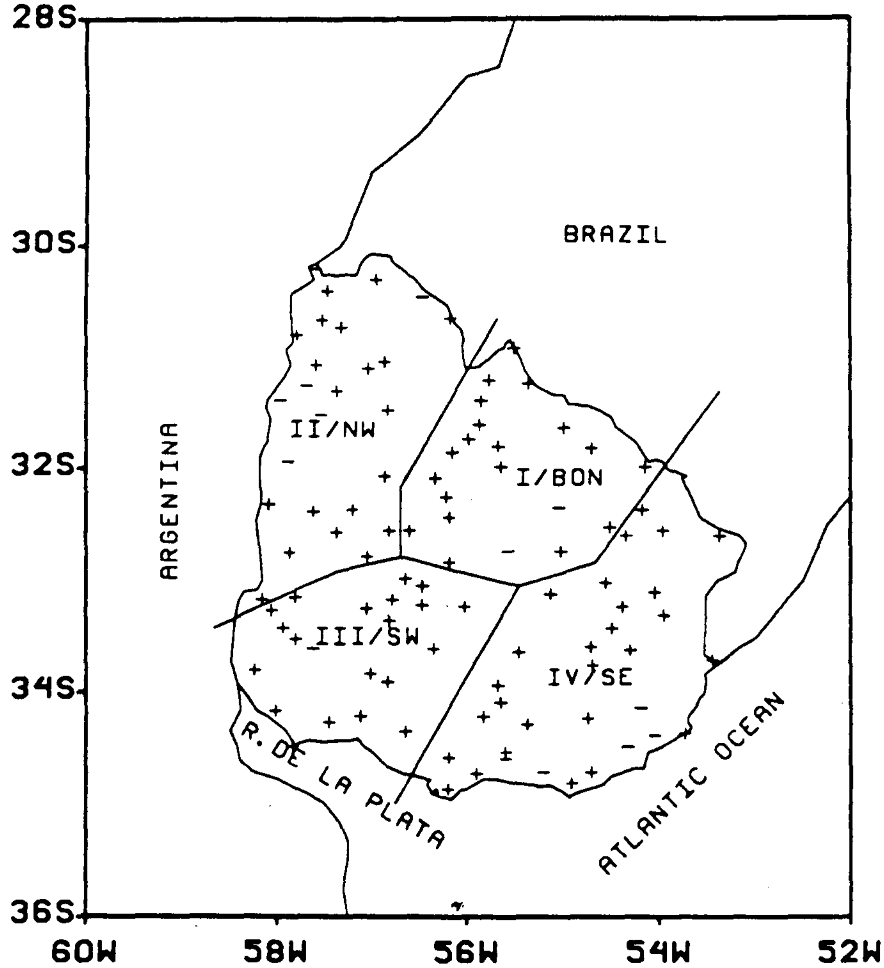

FIG. 1. Network of rainfall stations used in this study. Minus signs indicate the 13 rainfall stations with records that start after 1914 (between 1915 and 1931); plus signs indicate the 86 rainfall stations with records that start before or in 1914.

ing to Fig. 3a, austral fall is the rainiest season in northwest Uruguay. The dominance of the semiannual harmonic in the climatological rainfall regime for northwest Uruguay—which extends to northeast Argentina, eastern Paraguay, and parts of southern Brazil—is evidence of a transitional regime that includes winter maritime rains and subtropical summer rains (Hsu and Wallace 1976; Prohaska 1976). The rainfall in the more maritime southern and eastern sectors shows a less pronounced annual cycle (Figs. 3b and 3c). The eastern sector (Fig. 3b) shows a weak maximum during winter. Despite the relatively small area of Uruguay, therefore, differences in the precipitation regimes between ocean and inland sectors are readily apparent.

Note in Fig. 2 that the ratio between standard deviation and mean value varies between 0.5 and 1.2, with most values near 1. This indicates a large interannual variability in the precipitation over the region. Most continental stations show a clear maximum in interannual variability around the austral fall. The existence of this maximum has not been previously documented to our knowledge.

4. Spatial structure of precipitation anomalies

In this section we analyze the rainfall data using the method described in RH86, RH87, and RH89. For each station, values of monthly precipitation are represented as a percentile rank by following a two-step procedure: 1) each month in the n-year record is ranked from 1 (for the smallest value of precipitation) to n (for the largest value) with repeated values being assigned consecutive ranks and 2) the ranked precipitation values are normalized by the number of years in the record and multiplied by 100. These percentile rank values allow comparisons among stations with different means and variances and facilitate interpretation of spatial patterns obtained by using data from stations with differences in those statistics. The problem of repeated months without data, which causes difficulties

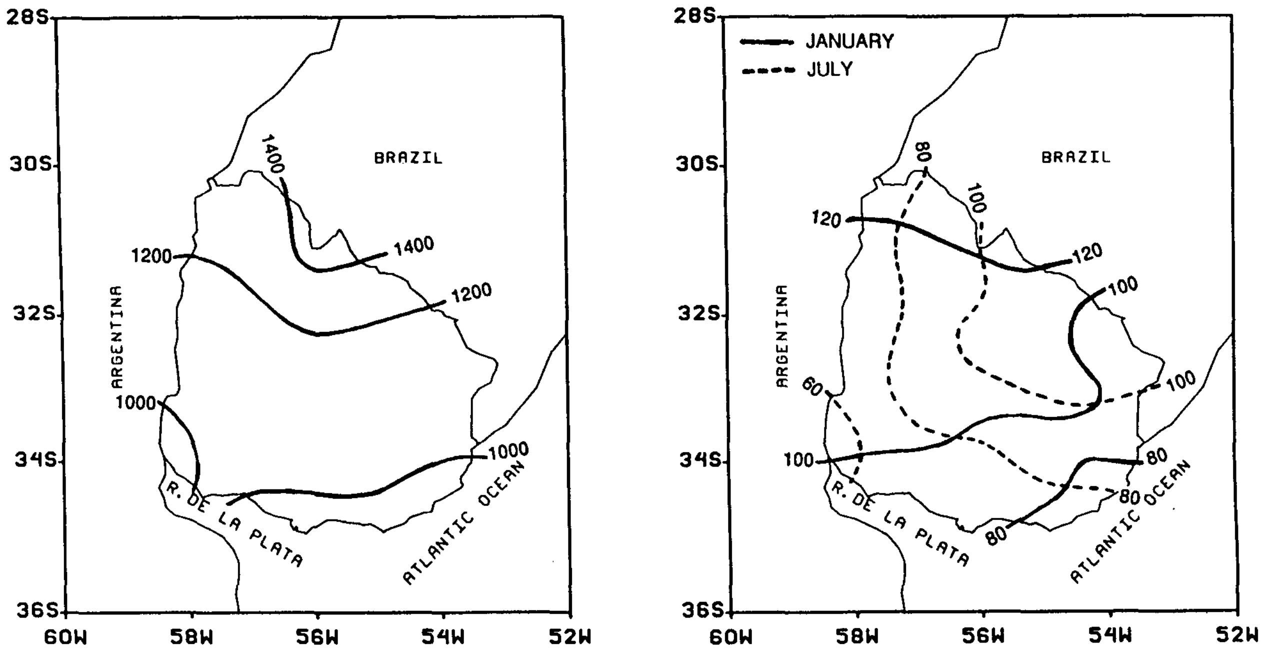

FIG. 2. Contour plot of annual-mean rainfall (left) and monthly mean rainfall for January and July (right); January: solid lines, July: dashed lines. Units are in millimeters.

in the ranking procedure as mentioned by RH87, does not appear in our dataset.

We consider separately the EN and HSOI years defined earlier in this paper (see Table 1). To start, we obtain two composite biennia for each rainfall station by averaging corresponding monthly percentile ranks in the period from July before to June after each EN and HSOI year, as in Rasmusson and Carpenter (1982) and Rasmusson and Wallace (1983). Each composite generally has more than ten components for most stations. Next, we determine the first Fourier harmonic for each composite biennium. Figures 4 and 5 show the amplitude and phase of this first harmonic for EN and HSOI events. We use a vector representation similar to that adopted by RH87 with different rules for EN and HSOI because we expect wet anomalies in the former events and dry anomalies in the latter events. If n is the number of years in the record, it can be shown that if the mean rainfall in the biennium is larger (smaller) than $50 + 50/n$, then the period around the month when the maximum (minimum) of that first harmonic is reached is of wet (dry) anomalies. These conditions are met at almost all stations.

Figures 4 and 5 show a strong tendency for wet anomalies around December of EN years and for dry anomalies around November of HSOI years. To obtain indexes of spatial coherence we compute the ratio between the amplitude of the vector sum for every station and the sum of the amplitudes of vectors for all stations. For Uruguay, the index of spatial coherence is high for both EN and HSOI events (see the left-hand column of Tables 2 and 3). These results are in agreement with RH87 and RH89, even though the calculations reported in those studies are carried out for a much larger region and with far fewer stations. Figures 4 and 5 also show that rainfall anomalies for both EN and HSOI are relatively more intense and coherent in the northern and central parts of Uruguay than in the maritime–oceanic southern regions.

5. Spatial composite biennia and time series analysis

The results presented in section 4 of this paper suggest both regional coherence and subregional differences. In this section, we divide Uruguay into subregions according to differences in precipitation regimes, hydrological interest, and suggestions from earlier studies on the regional climate (see Fig. 1). The northern part of the region is divided into two subregions: (i) the basin of the artificial lake of Rincón de Bonete, which is selected because rainfall anomalies can influence the generation of electric power in three hydroelectric plants on the Negro River (subregion I-BON), and (ii) the northwestern sector (subregion II-NW), whose precipitation regime shows continental influences with a double peak in the seasonal cycle (see section 2). Note that the results corresponding to subregion I-BON and, to some extent, those of the subregion II-NW, can be directly contrasted with those obtained by Mechoso and Pérez (1992). The southern part of the region is also divided into two subregions: (i) the southwestern sector (subregion III-SW), which is expected to be representative of a transitional regime between the mostly continental and maritime regimes,

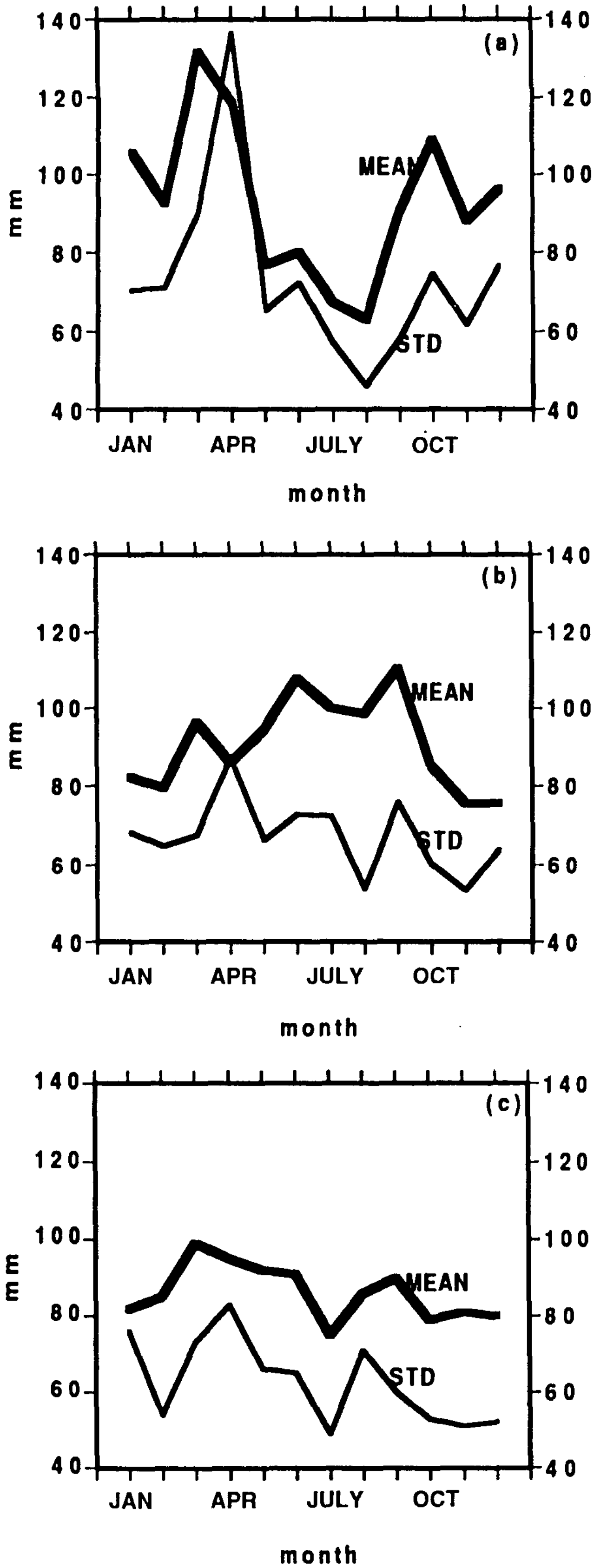

and (ii) the southeastern sector (subregion IV-SE), whose precipitation regime shows maritime influences with a weak maximum during winter in the seasonal cycle (see section 2). The results presented in this section were obtained by using the records from 86 stations for the period 1914–1977. For Uruguay and its four subregions the index of spatial coherence and averaged amplitude and phase of the vectors represented in Figs. 4 and 5 are given in Tables 2 and 3.

To perform our analysis we first obtain a time series of monthly precipitation percentiles for each station within the region for each calendar month. The procedure is based on fitting gamma distributions with "shape" and "scale" parameters estimated by using the method of moments (Ropelewski et al. 1985). We acknowledge that this may not be the most efficient way to obtain such estimates (Thom 1958), but efficiency is not an important consideration for the range of shape values (3 to 4) and sample sizes (around 60 or more) considered here. Precipitation is expressed as percentiles of a gamma distribution because these are easier to interpret and relate to physical processes than percentile ranks while maintaining some of the more desirable features of the percentile ranks. For example, both percentiles of a gamma distribution and percentile ranks effectively remove the annual cycle from the time series.

Our second step is to construct "aggregate" composites for each subregion of the monthly percentiles for the biennia starting in EN (or HSOI) years. We also construct EN and HSOI composite biennia for Montevideo by using data for the period 1883–1980. We focus on the periods with percentiles consistently above 50 for EN composite biennia and below 50 for HSOI composite biennia.

The EN and HSOI composite biennia obtained in this way are shown in Fig. 6. These composites confirm that Uruguay tends to have above average rainfall during EN events from the first November through the following January and, to a lesser extent, from the second March through the following July (Fig. 6a). This is particularly clear in the northern subregions I-BON and II-NW (Figs. 6c and 6e). On the other hand, the tendency is weak or almost disappears in the southern subregions III-SW and IV-SE (Figs. 6g and 6i) as well as in Montevideo (Fig. 6k), especially from the second March through the following July. The composite biennia also show that Uruguay tends to have below average rainfall during HSOI events from the first October through the following December, as well as from the second March through the following July (Fig. 6b).

FIG. 3. Annual cycle of monthly mean and standard deviation of precipitation at three selected meteorological stations: (a) Salto (31°23′S,57°58′W), (b) Melo (32°22′S,54°11′W), and (c) Montevideo (34°52′S,56°12′W).

TABLE 1. List of the ENSO years included in this study, identified as EN after Rasmusson and Carpenter (1983), and years during which the Tahiti–Darwin Southern Oscillation index remained in the upper 25% of the distribution for five months or longer, identified as HSOI years after Ropelewski and Jones (1987).

EN
1884, 1887, 1891, 1896, 1899, 1902, 1905, 1911, 1914, 1918, 1923, 1925, 1930, 1932, 1939, 1941, 1951, 1953, 1957, 1965, 1969, 1972, 1976
HSOI
1886, 1889, 1892, 1904, 1909, 1910, 1916, 1917, 1924, 1928, 1938, 1950, 1955, 1956, 1964, 1970, 1971, 1973, 1975

This is particularly clear in the southern subregions III-SW and IV-SE, as well as in Montevideo (Figs. 6h, 6j, and 6l). In both EN and HSOI events, the anomalies virtually disappear for a short period during one or two months at the beginning of the second year.

For SSA, RH87 and RH89 find wet anomalies during EN years from November through the following February and dry anomalies during HSOI years from June through December. The methodology used in those studies assumes that there is only one period with strong and persistent anomalies during the biennium. There is no particular reason to expect this a priori. For long-term forecasting, the period March–July after both EN and HSOI years is very interesting. For SSA, RH87 does not show important deviations from the 50th percentile from March through July after EN years. RH89, on the other hand, obtain percentiles below 50 from March through June—this is the last month included in their analysis—after HSOI years that can be even lower than those from June through December in HSOI years (see Fig. 12 in RH89). This

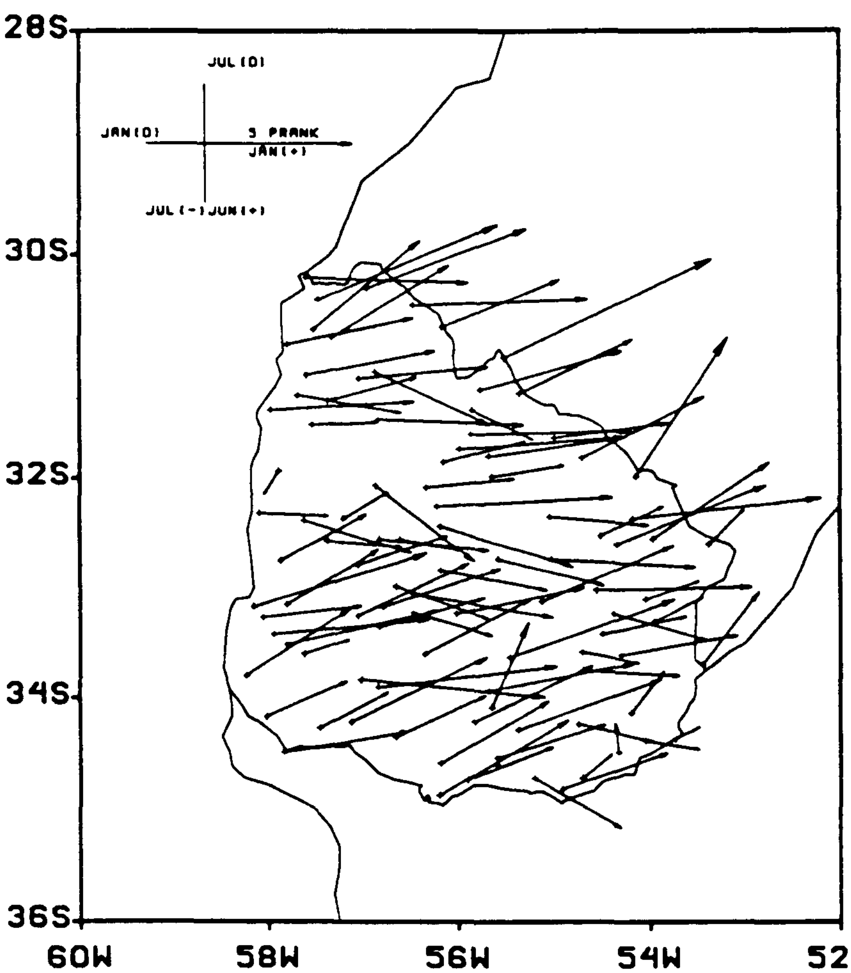

FIG. 4. Amplitude and phase of the first harmonic in monthly percentile ranks of precipitation in the biennia from the July before to the June after EN years. A horizontal vector pointing to the right indicates a *maximum* of the first harmonic in January after an EN year, with time increasing clockwise.

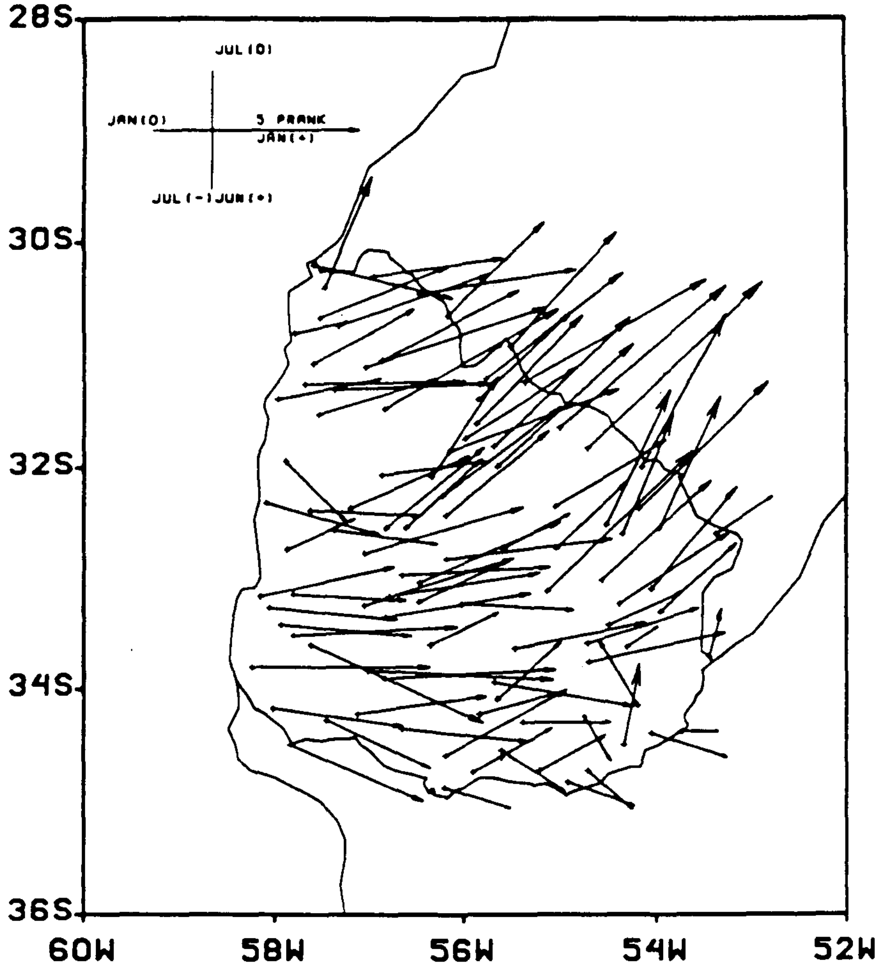

FIG. 5. As in Fig. 4 except for HSOI years. A horizontal vector pointing to the right indicates a *minimum* of the first harmonic in the January after an HSOI year, with time increasing clockwise.

difference between our results and those of RH87 could be at least partially due to compensation between anomalies in Uruguay and the rest of SSA. We cannot gain further insight into this issue with the dataset available for our study.

Figures 7, 8, and 9 show the time series of precipitation percentiles for Uruguay, its four subregions, and Montevideo for the two relevant periods in both cases. Namely, for EN events we consider the periods from November of EN years through the following January, and from March through July after EN years; for HSOI

TABLE 2. Index of spatial coherence for precipitation anomalies in Uruguay and its four subregions.

	Region				
	UY	I-BON	II-NW	III-SW	IV-SE
Number of stations	99	21	26	21	31
Spatial coherence index	0.943	0.947	0.937	0.967	0.936
Percentile rank amplitude vectorial mean	3.63	3.89	3.75	3.88	3.20
Phase in peak data [mo/day (approx)]	12/07	12/13	12/15	12/05	11/24

TABLE 3. As in Table 2 except for HSOI years.

	Region				
	UY	I-BON	II-NW	III-SW	IV-SE
Number of stations	99	21	26	21	31
Spatial coherence index	0.902	0.975	0.943	0.971	0.844
Percentile rank amplitude vectorial mean	3.87	5.04	4.14	4.57	2.81
Phase in peak date [mo/day (approx)]	11/17	10/09	12/01	12/30	12/07

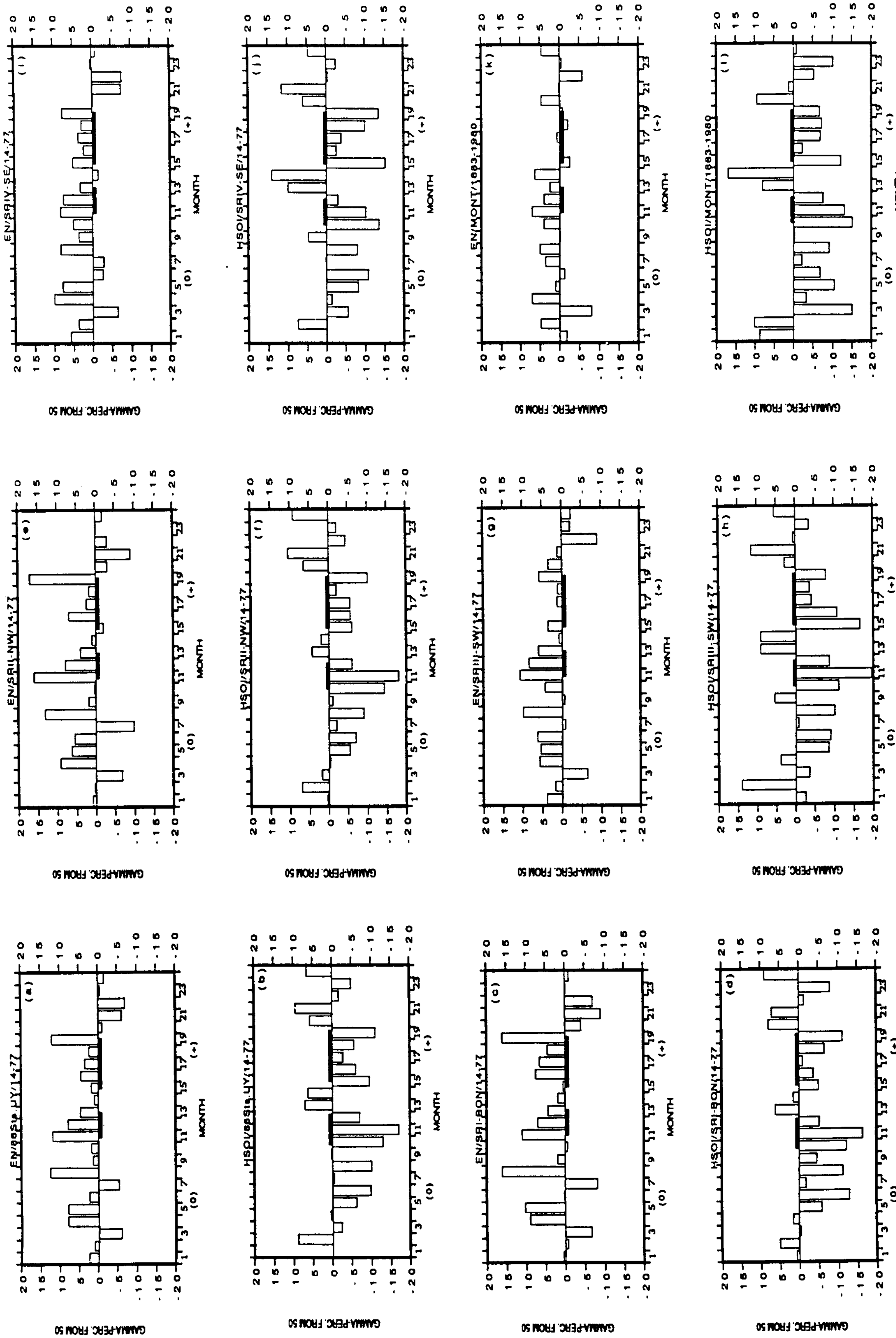

FIG. 6. Composite precipitation index (average gamma percentile) for EN biennia and for HSOI biennia: (a) and (b) spatial aggregates for Uruguay (86 stations, 1914–1977); (c) and (d) subregion I–BON (19 stations, 1914–1977); (e) and (f) subregion II–NW (20 stations, 1914–1977); (g) and (h) subregion III–SW (20 stations, 1914–1977); (i) and (j) subregion IV–SW (27 stations, 1914–1977); and (k) and (l) Montevideo (1883–1980). Black horizontal bars indicate the periods selected to analyze EN- or HSOI-related precipitation.

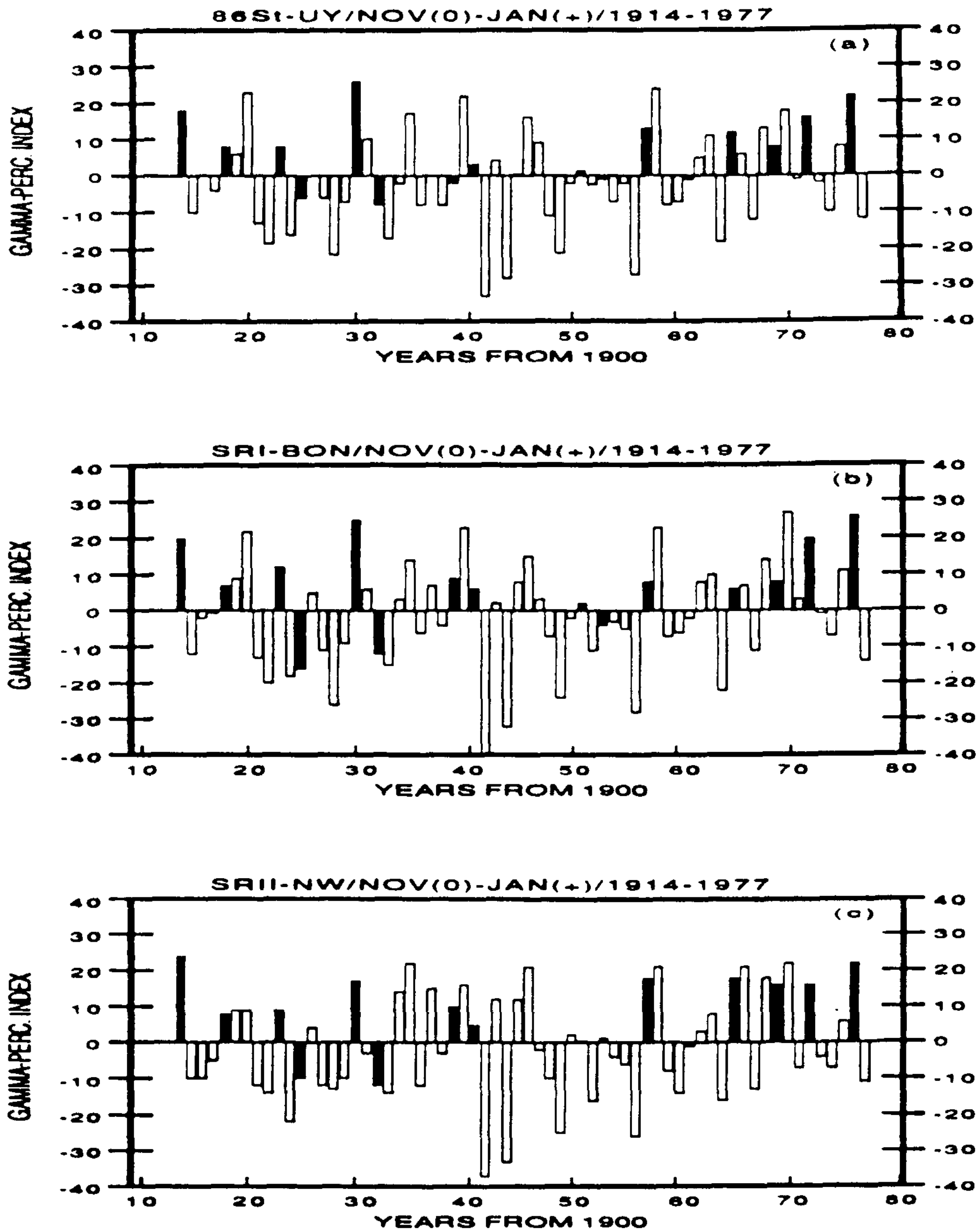

FIG. 7. Time series for the period November through the following January of the deviation from 50 of the precipitation index (average gamma percentile of station precipitation within the region or subregions) for (a) Uruguay; (b) subregion I-BON; (c) subregion II-NW; (c) subregion III-SW; (d) subregion IV-SE; and (e) Montevideo. The black bars represent EN years.

events we consider October through December of HSOI years, and March through July after HSOI years. Figures 7, 8, and 9 confirm that precipitation anomalies in those periods are predominantly positive during EN events and predominantly negative during HSOI events. The figures also show that precipitation anomalies from the second March through the second July tend to be weak or disappear in the southern subregions during EN events but not during HSOI events.

Note that there can be positive precipitation anomalies in years without EN events and negative precipitation anomalies in years without HSOI events. This is evidence that the SO is not the only factor influencing precipitation. It is clear that other phenomena can influence the interannual variability of precipitation in Uruguay. Examples of these phenomena include oceanic and atmospheric anomalies in the South Atlantic sector. Also note that there can be dry anomalies

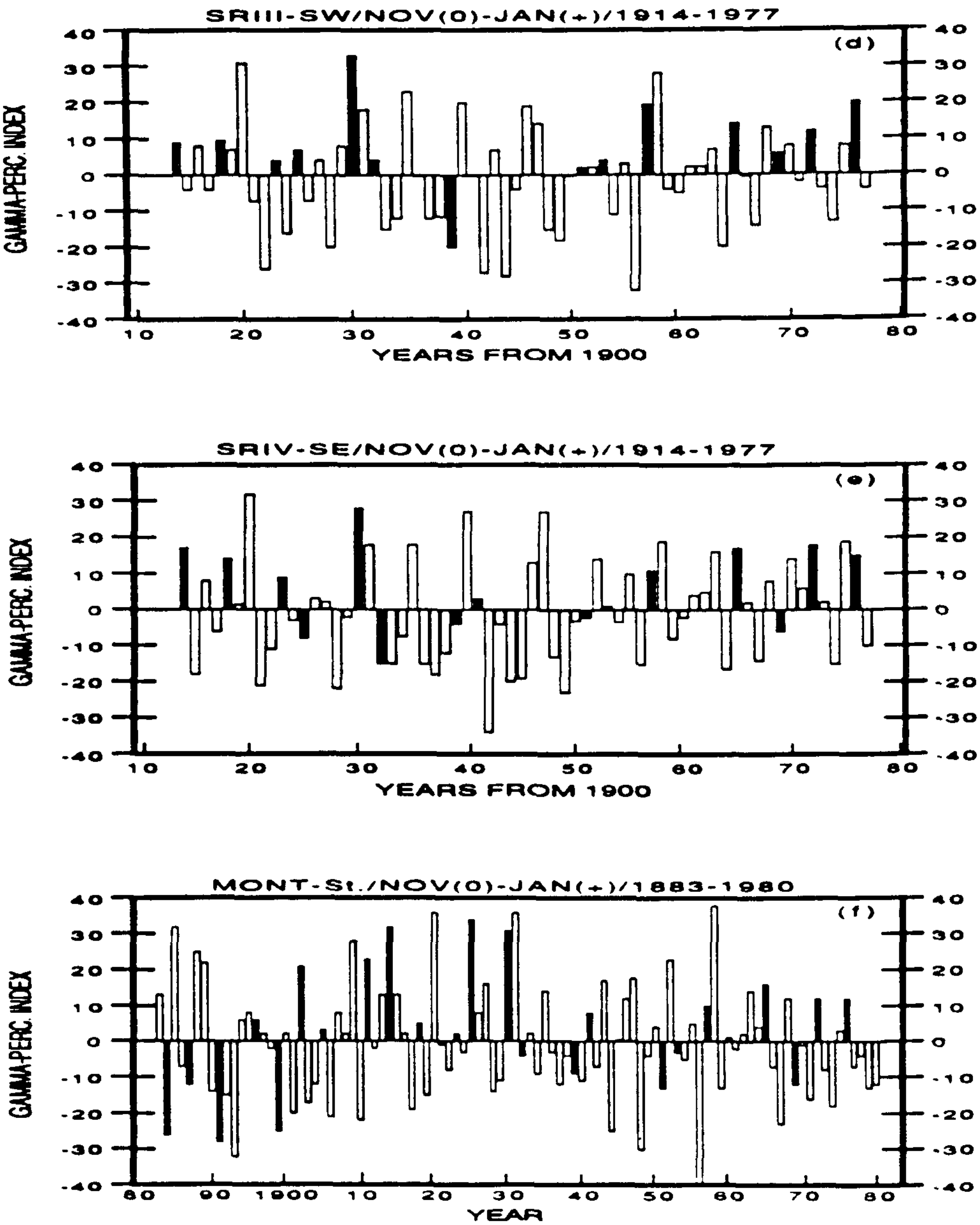

FIG. 7. (*Continued*)

in years with EN events (e.g., 1925) and wet anomalies in years with HSOI events (e.g., 1970). However, there are neither severe droughts during EN events nor strong floods during HSOI events.

We next assess the statistical significance of the relationships between the SO and rainfall discussed so far. We test the hypothesis that the relevant periods are especially wet during EN events and especially dry during HSOI events. To this effect we use the hypergeometric distribution (Feller 1957), as in RH89. The results of this calculation are shown in Tables 4 and 5. Note that the statistical significance of the results decreases in the southern part of Uruguay during EN events, but not during HSOI events. This may be part of a larger-scale feature that extends southwest toward Argentina. For HSOI events, both relevant periods are significantly dry. On the other hand, there are no significant anomalies during the period from March through July after EN years (see Fig. 9 and Table 4). This is further evidence that the physical mechanisms at work to produce rainfall anomalies during each extreme phase of the SO may be substantially different. The results for Montevideo are particularly interesting, since the significance level found for the period from November of EN years through the next January (0.86) is lower than any of the other regional values. This is

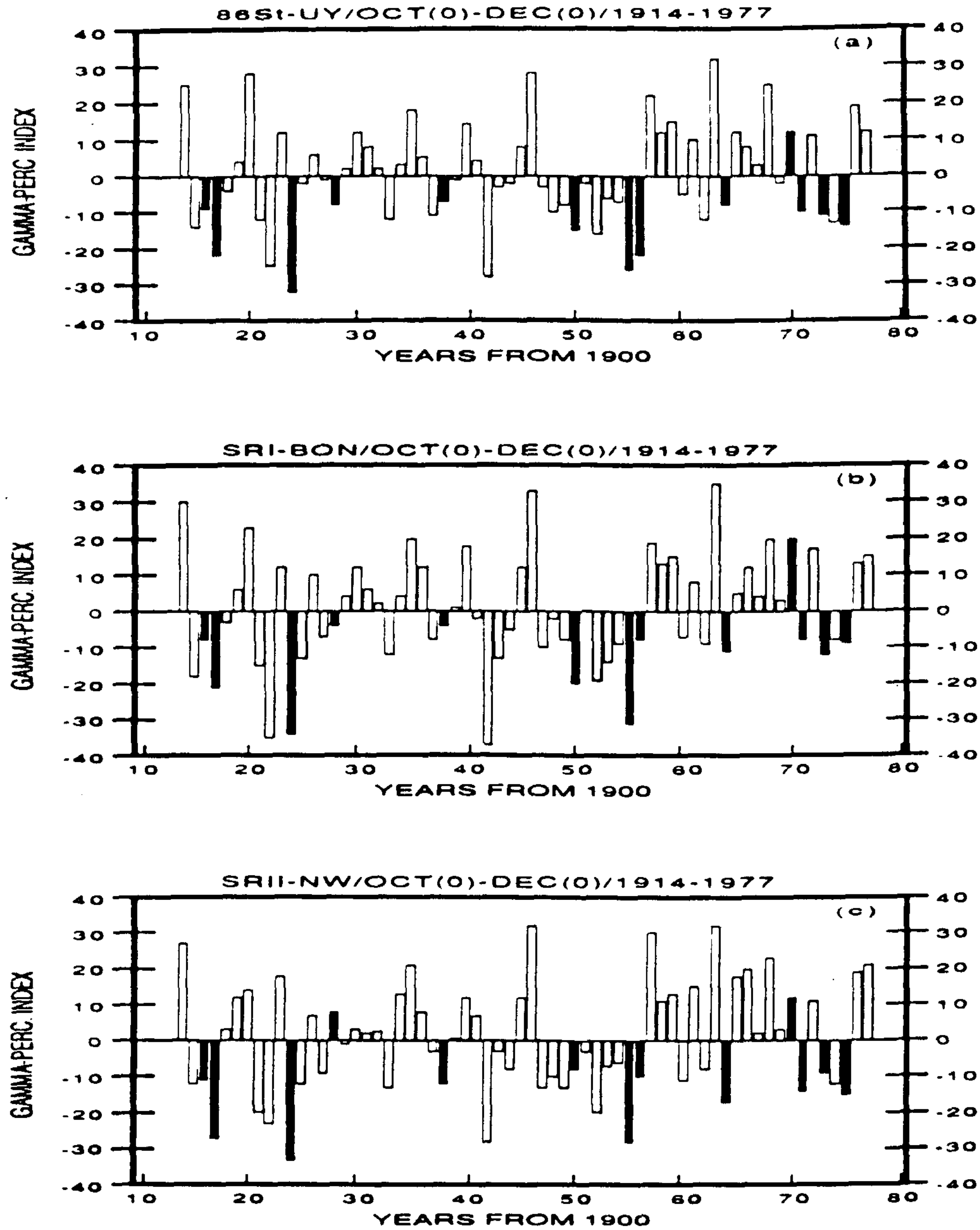

FIG. 8. As in Fig. 7 except for the period from October through the next December. The black bars represent HSOI years.

expected because precipitation records for individual stations have high frequency variations that are smoothed by spatial averages.

An interesting feature shown in Fig. 6 is that rainfall anomalies during January–February after HSOI years, particularly in the southern part of Uruguay, can be positive with percentiles clearly above 50. In fact, the percentiles for Montevideo reach 67 during February. This feature does not have a counterpart in EN biennia, which show an interruption of the significant anomalies in February of the second year but not opposite in sign. To further explore this issue, Fig. 10 shows the rainfall anomalies during November of HSOI years and during the following February and March for Montevideo, where the mean monthly rainfall is approximately 100 mm (see Fig. 2). Note in Fig. 10 that November and March tend to have below average rainfall, but that February tends to have above average rainfall. Evidence of this phenomenon for SSA is presented in RH89 as indicated above. Aceituno (1988) finds positive outgoing longwave radiation (OLR) anomalies in SSA during November–December 1975 and March–April

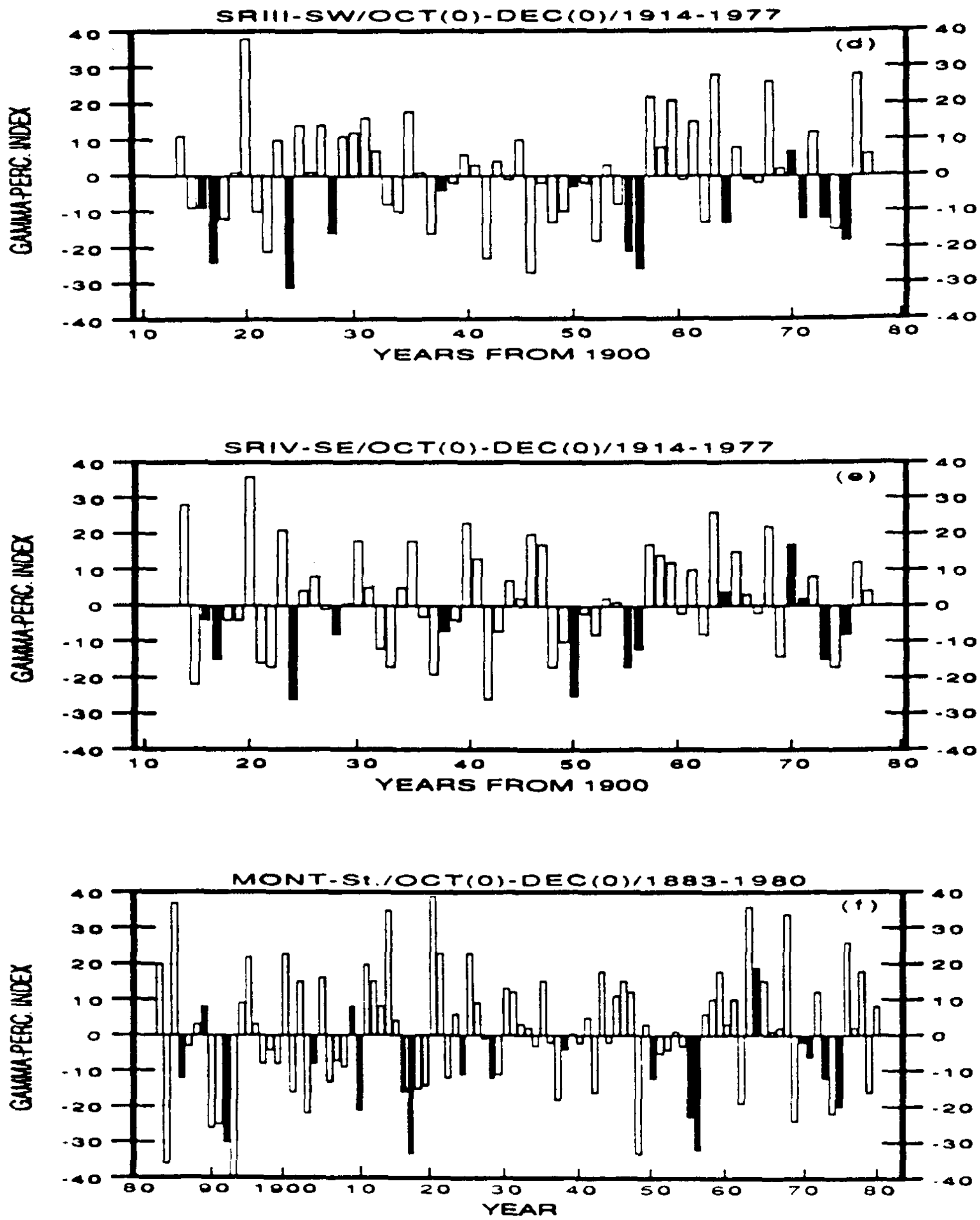

FIG. 8. (*Continued*)

1976, consistent with dry anomalies in those periods. During January–February 1976, on the other hand, there are negative OLR anomalies in SSA. Similar patterns are found by inspection of OLR anomalies for the 1988 HSOI event published by the Climate Analysis Center (Kousky 1988). The variations in the streamflow of the Paraná River show a similar behavior (Aceituno 1991).

More work is needed to better understand the behavior of rainfall anomalies in the early months after HSOI years. It is tempting to speculate that this behavior is due to the stronger midsummer effects of heating associated with a continental mass under clear skies. This would generate a stronger monsoonlike circulation, particularly since the zonal circulation is weaker, which would be associated with higher precipitation over the continent. In the austral midsummer of HSOI years, therefore, local effects that produce rain would override large-scale effects that produce drought. As the summer advances and the sun returns to the Tropics, large-scale effects become dominant again. The generation of wavelike patterns over eastern South America by the combined effects of diabatic heating over the continent and the tropical Pacific was demonstrated by Semazzi (1989) and Kalnay et al. (1986). These wavelike pat-

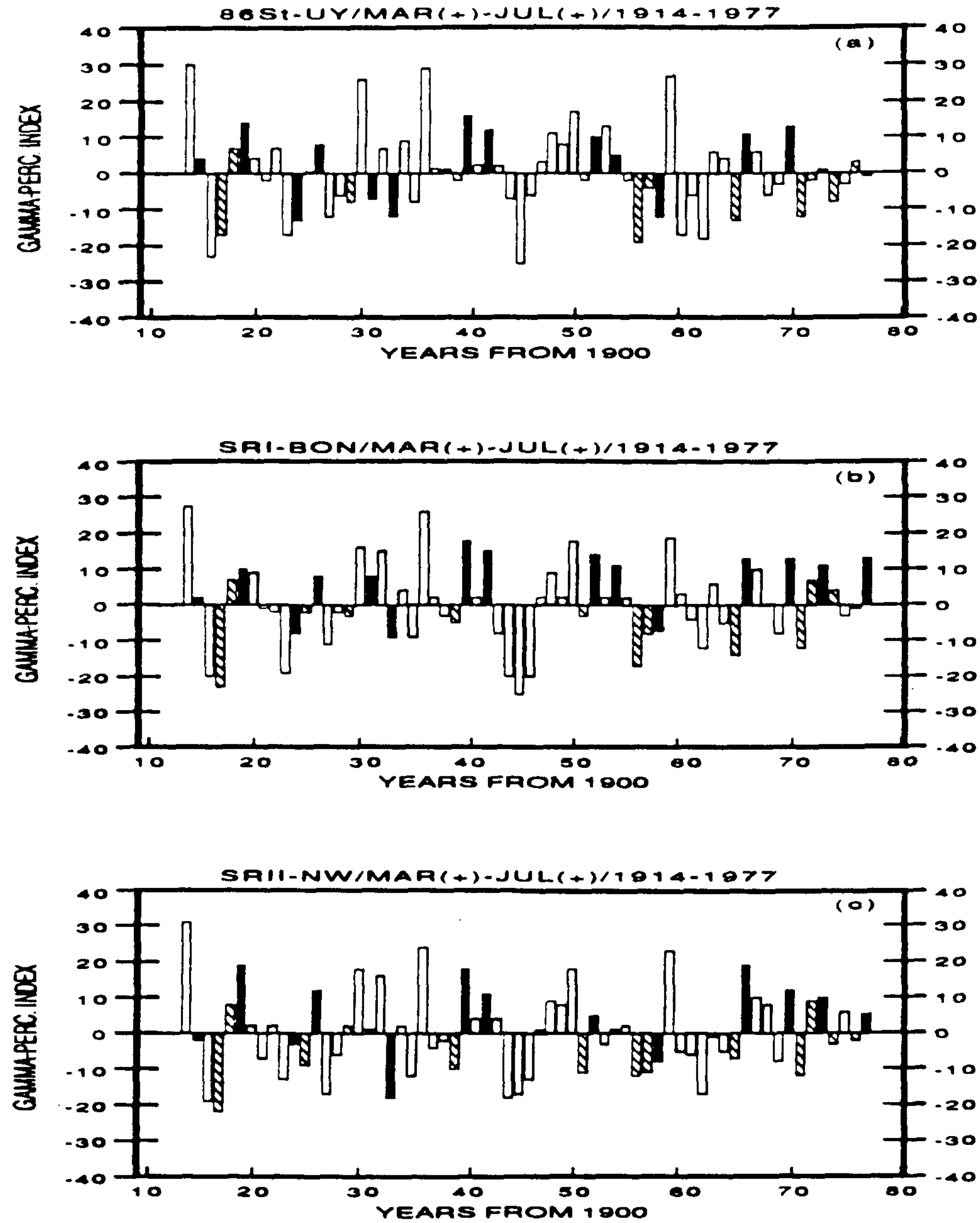

FIG. 9. As in Fig. 7 except for the period from March through July. The black bars represent years after an EN year, and the crossed bars represent years after an HSOI year.

terns would be consistent with the alternate sign of OLR anomalies observed in eastern South America during HSOI events.

6. Summary and conclusions

We have examined long records of monthly precipitation from a dense network of stations in Uruguay and analyzed the spatial and temporal relationships between rainfall anomalies and the extreme phases of the SO. Our results are in broad agreement with those obtained in previous studies that have included the region. We provide a more accurate description of these relationships regarding their spatial range and temporal development, as well as some new findings. We emphasize the following results:

- There is a very significant tendency for above average precipitation from November of EN years through the next January, particularly in the northern and western parts of Uruguay. For this period, wet anomalies are strongest in the northern part.

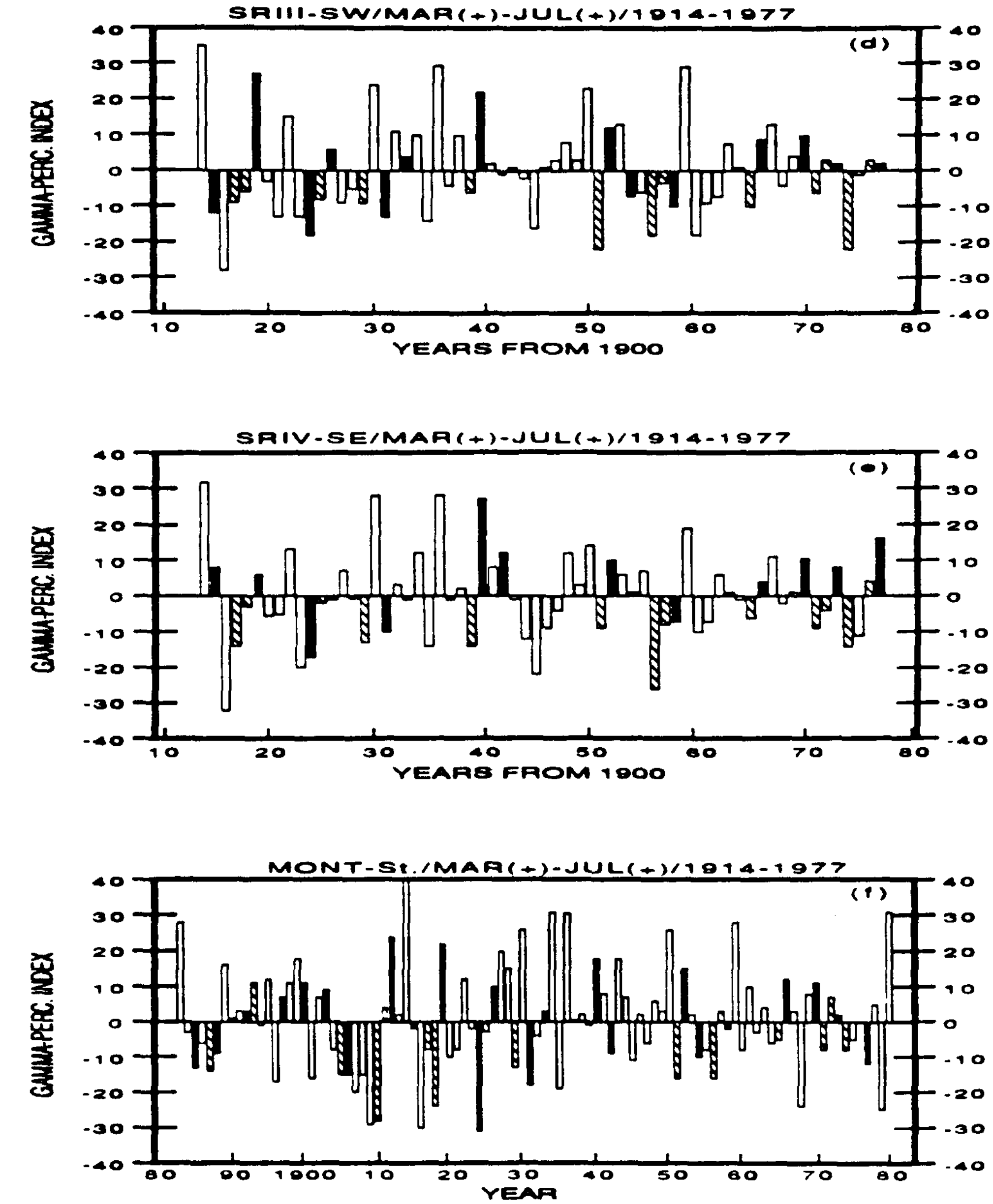

FIG. 9. (*Continued*)

• There is a very significant tendency for below-average precipitation from October through December of HSOI years in all of Uruguay. The strongest negative anomalies during this period are larger in magnitude than the strongest positive anomalies for EN events.

• There are no dry anomalies during January and February after HSOI years. In fact, there are positive anomalies, particularly in the southern part of Uruguay. This sign reversal does not have a symmetric counterpart after EN years.

• There are highly significant positive and negative precipitation anomalies from March through July of the year following an EN or HSOI year, respectively, in the northern part of Uruguay. For EN events, there is a weak tendency for wet anomalies in the southern maritime subregions. For HSOI events, the tendency for dry anomalies is also statistically very significant in the southern maritime subregions. RH89 did not emphasize the dry anomalies in SSA during the period March–July after HSOI years, although this feature can be seen in their results.

These results for Uruguay confirm the spatial and temporal asymmetries in the rainfall anomalies associated with the two extremes of the SO cycle identified for SSA in RH87 and RH89. These asymmetries char-

TABLE 4. Statistical significance of EN-related precipitation anomalies for Uruguay and its four subregions (see Fig. 1), and for Montevideo. The hypothesis tested is whether the periods indicated are wetter than normal during EN events.

	Number of EN events			
	Total	Wet	Dry	Significance
November of EN year through the next January				
Uruguay (86 stations)	15	11	4	0.99
SRI—BON (19 stations)	15	12	3	0.99
SRII—NW (20 stations)	15	13	2	0.99
SRIII—SW (20 stations)	15	13	2	0.99
SRIV—SE (27 stations)	15	10	5	(0.88)
Montevideo	23	14	9	(0.86)
March after EN year through next July				
Uruguay (86 stations)	15	10	5	(0.85)
SRI—BON (19 stations)	15	12	3	0.98
SRII—NW (20 stations)	15	11	4	0.96
SRIII—SW (20 stations)	15	9	6	(0.77)
SRIV—SE (27 stations)	15	10	5	[0.93]
Montevideo	23	13	10	(0.65)

acterize this region from others in the world where positive and negative anomalies are associated with EN or HSOI events during the same period (relative to the event) and with a similar spatial pattern (RH87, RH89). These characteristics do not allow us to study this problem using an approach based on either linear models or statistics.

The regional features in anomalous precipitation reviewed and described in this paper are an integral part of large-scale patterns affecting southeastern South America. Several studies on the anomalous large-scale circulation (particularly over South America) during extremes of the SO (e.g., Karoly 1989; Aceituno 1989; Kousky et al. 1984; Arkin 1982) show many well-established features that suggest teleconnections between the equatorial Pacific and the SSA, and the physical mechanisms involved in these teleconnections (RH89; Kousky and Ropelewski 1989). However, little is known about the physical mechanisms that produce the anomalous patterns described in this paper and that determine their timing. This is not so in other regions of South America [see the study of Rutllant and Fuenzalida (1991) for central Chile].

To understand the relationships between events in the equatorial Pacific and the SSA, one should consider anomalous circulations associated with each phase of the SO both in the large scale and the regional scale. At the regional-scale level, Velasco and Fritsch (1987) show large differences between the convective activity over midlatitude South America between an EN year (summer 1982/83) and a non-EN year (summer 1981–1982). These differences, whose significance has to be confirmed by more case studies, might contribute to an explanation of some of the results reported here as well as in previous studies. For example, we find that there are no significant rainfall anomalies during late summer (February after an EN year). If the subtropical jet stream plays a key role in the teleconnections, its monthly mean position must be important to determine the affected regions. During February, the jet stream in the Southern Hemisphere is in its southernmost location, which is south of Uruguay. This could explain the transient disappearance of SO-related anomalies in this particular subregion of SSA.

Aceituno (1988) finds that the convective band that extends from the Amazon Basin to the South Atlantic shows remarkably coherent OLR anomalies during periods of strong positive and negative SO phase during the austral summer. He suggests that aspects in the interannual variability of rainfall in SSA and the Paraná River discharge could be associated with those anomalies in convective activity. He indicates that there might be interesting relationships between those SO-related anomalies in convective activity and cold front incursions into tropical portions of Brazil (see also Kousky 1979). It is known that midlatitude frontal systems play a very important role in determining the amount of precipitation in southeastern South America (Prohaska 1976; Ratisbona 1976). There is no evidence, however, of any clear relationship between the number of frontal passages for the 10-year period 1961–1970 (Kousky 1979, see Table 1) and the extremes of the SO.

We suggest that the interannual variability in the tropical Pacific Ocean is an important contributor to the interannual variability of precipitation in Uruguay.

TABLE 5. As in Table 4 except for HSOI. The hypothesis tested is whether the periods are drier than normal during HSOI events.

	Number of HSOI events			
	Total	Wet	Dry	Significance
October of HSOI year through next December				
Uruguay (86 stations)	13	1	12	0.98
SRI—BON (19 stations)	13	1	12	0.99
SRII—NW (20 stations)	13	2	11	0.99
SRIII—SW (20 stations)	13	1	12	0.99
SRIV—SE (27 stations)	13	3	10	0.97
Montevideo	19	3	16	0.99
March after HSOI year through next July				
Uruguay (86 stations)	13	3	10	0.98
SRI—BON (19 stations)	13	3	10	0.98
SRII—NW (20 stations)	13	3	10	0.97
SRIII—SW (20 stations)	13	2	11	0.99
SRIV—SE (27 stations)	13	1	12	0.99
Montevideo	19	6	13	0.95

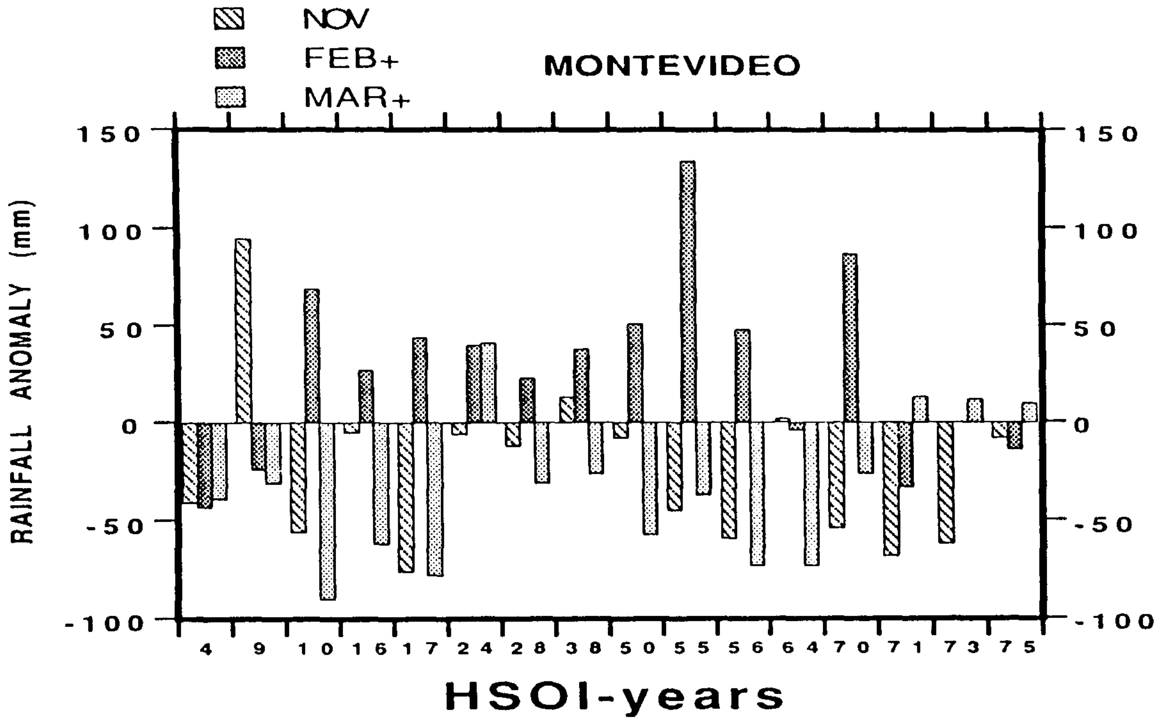

FIG. 10. Rainfall anomalies in Montevideo associated with HSOI years.

Our results suggest that to better understand the development of rainfall anomalies over SSA we should consider the relationships between large-scale circulation patterns, frontal activity, and regional-scale convective features. In addition, we should consider the variability in the atmosphere and ocean circulations in the South Atlantic sector. This is because the water vapor source for this region is the South Atlantic Ocean, and the moisture from tropical South America (Prohaska 1976; Wang et al. 1992) and SSA is directly affected by the South Atlantic anticyclonic circulation.

Acknowledgments. We wish to thank R. Guarga and J. L. Genta from IMFIA for their encouragement during the course of this study. Special thanks are due to C. Konor (at UCLA) and C. M. Anido (at IMFIA) for technical help. We are very grateful to J. Fontana, J. Patrone, and A. Tozzo of Usinas y Trasmisiones Eléctricas-Uruguay for their support. K. Mah typed the manuscript. This research was supported by Usinas y Trasmisiones Eléctricas-Uruguay and by the National Science Foundation under Grant ATM 9122/53.

REFERENCES

Aceituno, P., 1988: On the functioning of the Southern Oscillation in the South American sector. Part I: Surface climate. *Mon. Wea. Rev.*, **116**, 505–524.

——, 1989: On the functioning of the Southern Oscillation in the South American sector. Part II: Upper-air circulation. *J. Climate,* **2**, 341–355.

——, 1991: Anomalías climáticas en la región sudamericana durante los extremos de la Oscilación Austral. *II Cursos Latinoamericanos sobre Aspectos Meteorológicos y Oceanográficos del Fenómeno ENSO.* Departamento de Geofísica, Universidad de Chile, Santiago, 1–10.

Arkin, P. A., 1982: The relationship between interannual variability in the 200 mb tropical wind field and the Southern Oscillation. *Mon. Wea. Rev.*, **110,** 1393–1404.

Bidegain, M., and M. Caffera, 1989a: La variación en los días con precipitación en la región sureste de América del Sur (Uruguay). Departamento de Meteorología, Facultad de Ciencias, Universidad de la República, Montevideo, Uruguay, 9 pp. [Available from Dept. de Meteorología, Fac. de Ciencias, U. R. T. Narvaja 1676, Montevideo, Uruguay.]

——, and ——, 1989b: Anomalías de la precipitación en la región sureste de América del Sur (Uruguay) asociadas con el fenómeno de El Niño–Oscilación Sur. Departamento de Meteorología, Facultad de Ciencias, Universidad de la República, Montevideo, Uruguay, 5 pp. [Available from Dept. de Meteorología, Fac. de Ciencias, U. R. T. Narvaja 1676, Montevideo, Uruguay.]

Feller, W., 1957: *An Introduction to Probability Theory and Its Applications.* Vol. I., 2d ed. John Wiley & Sons, 461 pp.

Halpert, M., and C. F. Ropelewski, 1992: Surface temperature patterns associated with the Southern Oscillation. *J. Climate,* **5,** 577–593.

Hsu, C. F., and J. M. Wallace, 1976: The global distribution of the annual and semiannual cycles in precipitation. *Mon. Wea. Rev.,* **104,** 1093–1101.

Kalnay, E., K. Mo, and J. Peagle, 1986: Large-amplitude short-scale stationary Rossby waves in the Southern Hemisphere: Observations and mechanistic experiments to determine their origin. *J. Atmos. Sci.,* **38,** 252–275.

Karoly, D. J., 1989: Southern Hemisphere circulation features associated with El Niño–Southern Oscillation events. *J. Climate,* **2,** 1239–1252.

Kiladis, G., and H. Diaz, 1989: Global climatic anomalies associated with extremes in the Southern Oscillation. *J. Climate,* **2,** 1069–1090.

Kousky, V. E., 1979: Frontal influences on Northeast Brazil. *Mon. Wea. Rev.,* **107,** 1140–1153.

——, Ed., 1988: Climate Diagnostic Bulletin. Climate Analysis Center, October 1988 issue, 38 pp. (see also November and December 1988 and January, February, March, and April 1989).

——, and C. F. Ropelewski, 1989: Extremes in the Southern Oscillation and their relationships to precipitation anomalies with emphasis on the South American region. *Interciencia,* **14,** 325–337.

——, M. T. Kagano, and I. F. A. Cavalcanti, 1984: A review of the Southern Oscillation: Oceanic–atmospheric circulation changes and related rainfall anomalies. *Tellus,* **36A,** 490–504.

Lau, K. M., and P. J. Sheu, 1988: Annual cycle, quasi biennial oscillation, and Southern Oscillation in global precipitation. *J. Geophys. Res.,* **93**(D9), 10 975–10 988.

Mechoso, C. R., and G. Pérez-Iribarren, 1992: Streamflow in southeastern South America and the Southern Oscillation. *J. Climate,* **5,** 1535–1539.

Pittock, A. B., 1980: Patterns of climatic variation in Argentina and Chile. Part I. Precipitation, 1931–60. *Mon. Wea. Rev.,* **108,** 1347–1361.

Prohaska, F., 1976: The climate of Argentina, Paraguay and Uruguay. *Climates of Central and South America. World Survey of Climatology,* Vol. 12, W. Schwerdtfeger, Ed., Elsevier, 13–112.

Rasmusson, E. M., and T. H. Carpenter, 1982: Variations in tropical sea surface temperature and surface wind fields associated with the Southern Oscillation/El Niño. *Mon. Wea. Rev.,* **110,** 354–384.

——, and ——, 1983: The relationships between eastern equatorial Pacific sea surface temperatures and rainfall over India and Sri Lanka. *Mon. Wea. Rev.,* **111,** 517–528.

——, and J. M. Wallace, 1983: Meteorological aspects of the El Niño/Southern Oscillation. *Science,* **222,** 1195–1202.

——, X. Wang, and C. F. Ropelewski, 1990: The biennial component of ENSO variability. *J. Mar. Syst.,* **1,** 71–96.

Ratisbona, L. R., 1976: The climate of Brazil. Climates of Central and South America. *World Survey of Climatology,* Vol. 12, W. Schwerdfeger, Ed., Elsevier, 219–294.

Ropelewski, C. F., and M. S. Halpert, 1986: North American precipitation and temperature patterns associated with El Niño–Southern Oscillation. *Mon. Wea. Rev.,* **114,** 1101–1106.

——, and ——, 1987: Global and regional scale precipitation patterns associated with El Niño–Southern Oscillation. *Mon. Wea. Rev.,* **115,** 1606–1626.

——, and Jones, 1987: An extension of the Tahiti–Darwin Southern Oscillation index. *Mon. Wea. Rev.,* **115,** 2161–2165.

——, and M. S. Halpert, 1989: Precipitation patterns associated with the high index phase of Southern Oscillation. *J. Climate,* **2,** 268–284.

——, J. E. Janowiak, and M. S. Halpert, 1985: The analysis and display of real time surface climate data. *Mon. Wea. Rev.,* **113,** 1101–1106.

——, M. S. Halpert, and X. Wang, 1992: Observed tropospheric biennial variability and its relationship to the Southern Oscillation. *J. Climate,* **5,** 594–614.

Rutllant, J., and H. Fuenzalida, 1991: Synoptic aspects of the central Chile rainfall variability associated with the Southern Oscillation. *Int. J. Climatol.,* **11,** 63–76.

Semazzi, F., 1989: An investigation of the role of orography and thermal forcing in the Southern Hemisphere. *Extended Abstracts, Third Int. Conf. on Southern Hemisphere Meteorology,* Buenos Aires, Argentina, Amer. Meteor. Soc., 83–86.

Thom, H. C. S., 1958: A note on the gamma distribution. *Mon. Wea. Rev.,* **86,** 117–121.

Velasco, I., and J. M. Fritsch, 1987: Mesoscale convective complex in the Americas. *J. Geophys. Res.,* **92,** 9591–9613.

Wang, M., J. Paegle, and J. Nogues-Paegle, 1992: Moisture flux estimates in the vicinity of South America. *Proc. 16th Annual Climate Diagnostics Workshop,* Dept. of Atmospheric Sciences, University of California, Los Angeles; U.S. Department of Commerce, NOAA, NWS, 311–316.